https://doi.org/10.5194/esurf-2020-39
Preprint. Discussion started: 15 June 2020

Earth Surface Dynamics Discussions
Open Access
EGU

Transport-limited fluvial erosion – simple formulation and efficient numerical treatment

Stefan Hergarten[1]

[1]Institut für Geo- und Umweltnaturwissenschaften, Albertstr. 23B, 79104 Freiburg, Germany

Correspondence: Stefan Hergarten
(stefan.hergarten@geologie.uni-freiburg.de)

Abstract. Most of the recent studies modeling fluvial erosion in the context of tectonic geomorphology focus on the detachment-limited regime. One reason for this simplification is the direct relationship of the constitutive law used here – often called stream-power law – to empirical results on longitudinal river profiles. Another, not less important reason lies in the numerical effort that is much higher for transport-limited models than for detachment-limited models. This study proposes a simple formulation of transport-limited erosion that is as close to empirical results on river profiles as the stream-power law is. As a central point, a direct solver for the fully implicit scheme is presented. This solver requires no iteration for the linear version of the model, allows for arbitrarily large time increments, and is almost as efficient as the established implicit solver for transport-limited erosion. The numerical scheme can also be applied to linear models between the two extremes of detachment-limited and transport-limited erosion.

1 Introduction

Rivers play a major if not dominant part in large-scale landform evolution. If horizontal displacement of the crust is not taken into account, models describing the evolution of a topography $H(x_1, x_2, t)$ are typically written in the form

$$\frac{\partial H}{\partial t} = U - E, \tag{1}$$

where U and E are uplift rate and erosion rate, respectively.

Two limiting cases – detachment-limited and transport-limited erosion – are widely considered in the context of fluvial landform evolution. For detachment-limited erosion, it is assumed that all particles entrained by the river are immediately removed from the system. The erosion rate E can be considered as a function of local properties at each point. In the simplest approach, these are catchment size and channel slope (slope in direction of steepest descent), while all other influences are subsumed in a lumped parameter often called erodibility.

In all scenarios other than the detachment-limited case, a sediment balance must be considered. If no material is directly removed, the erosion rate is

$$E = \mathrm{div}\boldsymbol{q}, \tag{2}$$

https://doi.org/10.5194/esurf-2020-39
Preprint. Discussion started: 15 June 2020


Earth Surface Dynamics Discussions Open Access EGU

where $\boldsymbol{q}$ is the sediment flux density (volume per time and cross section length) and div the 2-D divergence operator. It is usually assumed that $\boldsymbol{q}$ follows the direction of the channel slope, so only its absolute value q varies between different models. Transport-limited models directly define the sediment flux density q instead of the erosion rate E at each point as a function of local properties such as catchment size and channel slope.

Mathematically, both concepts differ fundamentally. Equation (1) only involves derivatives of first order with regard to time and with regard to the spatial coordinates (arising from the channel slope) in the detachment-limited scenario. So it is a hyperbolic differential equation of the advection type. Propagation of information in one direction only – upstream here – is a characteristic property of this type. Anything that happens at a given point and a given time only affects the region upstream of this point in future. In contrast, Eq. (1) contains spatial derivatives of second-order in the transport-limited regime (from the channel slope and from the divergence operator). Equation (1) combined with Eq. (2) is a parabolic differential equation of the diffusion type then, where information propagates in both upstream and downstream direction.

Several comprehensive numerical models of fluvial landform evolution have been developed since the 1990s. All models reviewed by Coulthard (2001), Willgoose (2005), and van der Beek (2013) involve a sediment balance. In the last years, however, there seems to be a trend to the detachment-limited model, although the idea that all particles are immediately excavated is limited has been questioned (e.g., Turowski, 2012). All types of bedload transport are obviously not captured by this concept. Nevertheless, even some recent studies using models that are able to simulate sediment transport focus on the detachment-limited case (e.g., Duvall and Tucker, 2015; Theodoratos et al., 2018; Eizenhöfer et al., 2019).

At least three aspects make the detachment-limited approach appealing. First, there is a close relationship to old empirical studies of longitudinal channel profiles. Hack (1957) observed a power-law relationship between channel slope S and upstream catchment size A in several rivers. This relationship is nowaday often called Flint's law (Flint, 1974) and written in the form

$$S = k_s A^{-\theta}, \tag{3}$$

where θ is the concavity index and k_s the steepness index. Assuming that Eq. (3) is the fingerprint of a spatially constant erosion rate under uniform conditions, it can be assumed that

$$E = f(k_s) = f(A^\theta S), \tag{4}$$

where f is an arbitrary function. Assuming a power-law function,

$$f(k_s) = K k_s^n = K(A^\theta S)^n, \tag{5}$$

where the parameter K is denoted erodibility, has become some kind of paradigm in this context. The fluvial erosion rate is often written in the form

$$E = K A^m S^n \tag{6}$$

with $m = \theta n$. Equation (6) is often called stream-power law since it can be interpreted in terms of energy dissipation of the water per channel bed area if an empirical relationship between channel width and catchment size is used (e.g., Whipple and Tucker, 1999).

https://doi.org/10.5194/esurf-2020-39
Preprint. Discussion started: 15 June 2020


Earth Surface Dynamics Discussions
Open Access
EGU

The concavity index $\theta = \frac{m}{n}$ appears to be well constrained, so most modeling studies either use the value $\theta = 0.5$ originally found by Hack (1957) or a reference value $\theta = 0.45$ (e.g., Whipple et al., 2013; Lague, 2014). In turn, little is known about the exponent n since it cannot be constrained from the shape of equilibrium profiles under uniform conditions. The model is linear with regard to H (if the flow pattern is given) for $n = 1$, which simplifies both theoretical considerations and the numerical implementation. Thus, the lack of clear knowledge about n often serves as a reason for choosing $n = 1$. If θ is well constrained and $n = 1$ is accepted as a convenient choice, the erodibility K remains as the only parameter. It is a lumped parameter subsuming all influences on erosion other than channel slope and catchment size, so it is not only a property of the rock, but also depends on climate in a nontrivial way (e.g., Ferrier et al., 2013; Harel et al., 2016). However, it just defines how steep rivers will become at a given uplift rate, so reasonable values can be found, e.g., by analyzing river profiles at situations where estimates of the uplift rate are available.

The simplicity of the differential equation itself serves as a second argument in favor of the detachment-limited approach. In the linear case ($n = 1$), Eq. (1) combined with Eq. (6) can be solved analytically for any given uplift pattern and history. Disturbances propagate in upstream direction at a velocity KA^θ. The treatment can be simplified by the χ transform introduced by Perron and Royden (2013). It transforms the upstream coordinate x to a new coordinate

$$\chi = \int \left(\frac{A(x)}{A_0} \right)^{-\theta} dx, \tag{7}$$

where A_0 is an arbitrary reference catchment size and the integration starts from an arbitrary reference point. This transformation eliminates the inherent curvature of river profiles arising from the decrease of catchment size in upstream direction, so equilibrium profiles under spatially uniform conditions turn into straight lines. The solutions of this equation and their potential for unraveling the uplift and erosion history were investigated by Royden and Perron (2013), and a formal inversion procedure for the linear case ($n = 1$) was presented by Goren et al. (2014). So the detachment-limited model can be reconciled with real river profiles not only under steady-state conditions, but also in the context of temporal changes.

As a third, but despite increasing computing capacities still important point, detachment-limited erosion can be implemented in numerical models more efficiently than transport-limited erosion. Here, even a fully implicit scheme that allows for arbitrary time increments with linear time complexity, also known as $O(n)$, is available. This means that the computing effort increases only linearly with the total number of nodes. The scheme was introduced in the context of fluvial erosion by Hergarten and Neugebauer (2001), described in detail for $n = 1$ and $n = 2$ by Hergarten (2002), and made popular by Braun and Willett (2013).

So far there is no comparable implementation for transport-limited erosion. As mentioned above, transport-limited erosion corresponds to a diffusion-type equation. The challenge is that the diffusivity depends on the catchment size and thus varies over several orders of magnitude. Multigrid methods (e.g., Hackbusch, 1985) are still the only schemes for the diffusion equation in more than one dimension with linear time complexity. However, convergence breaks down if the diffusivity varies by some orders of magnitude, so multigrid methods have not been applied in the context of fluvial erosion. So far none of the existing landform evolution model treats the transport-limited case with a fully implicit scheme that allows for arbitrarily large time increments.

https://doi.org/10.5194/esurf-2020-39
Preprint. Discussion started: 15 June 2020


Earth Surface Dynamics Discussions
Open Access
EGU

The advantage of the detachment-limited model concerning the numerical complexity persists if explicit schemes are used here, too. The main reason for using explicit schemes for detachment-limited erosion is the artificial smoothing of knickpoints by the implicit discretization, while explicit schemes that preserve the shape of knickpoints better are available. A comparison was given by Campforts et al. (2017). As already pointed out by Howard (1994), explicit schemes for the transport-limited case typically require 3 to 4 orders of magnitude shorter time steps than for the detachment-limited case.

Howard (1994) already developed an approximation that makes the explicit scheme for the transport term numerically more stable. Kooi and Beaumont (1994) proposed an approach that increases stability and also allows for a physical interpretation, often called undercapacity model or – in a more general context – linear decline model (Whipple and Tucker, 2002). It defines an equilibrium flux density q_e from local properties (channel slope, catchment size, ...) and assumes that the erosion rate is

$$E = \frac{q_\mathrm{e} - q}{l}. \tag{8}$$

The parameter l defines a length scale and can be seen as inertia of sediment detachment and deposition against changes in fluvial conditions. The model consisting of Eqs. (1), (2), and (8) can be treated numerically by converting Eq. (2) to an integral equation based on the relation

$$Q = \int E \, dA, \tag{9}$$

where Q is the sediment flux (not flux density) and the integral extends over the upstream catchment of the considered point. Converting Q to a flux density and inserting it into Eq. (8) yields an integro-differential equation for the surface height H.

An alternative physical interpretation of the linear decline model was developed by Davy and Lague (2009). The detachment-limited model (Eq. 6) was extended by a sediment deposition term proportional to the actual sediment flux. As a main point, Davy and Lague (2009) found an expression for the rate of deposition that keeps equilibrium river profiles consistent with Eq. (3), which is not the case for the original undercapacity model (Whipple and Tucker, 2002).

Yuan et al. (2019) implemented an implicit numerical scheme for this model based on a Gauss-Seidel iteration in upstream direction. The convergence rate of the iteration was found to be independent of the size of the grid, so the scheme is indeed of linear time complexity. The rate of convergence, however, decreases for faster deposition and breaks down if the model approaches the transport-limited regime. It is therefore presumably the most efficient implementation of sediment transport in large-scale fluvial erosion models, but it still cannot come close to transport-limited regime.

In the following section, a formulation of transport-limited erosion is proposed that can be directly reconciled with the concept of the erodibility. Then, Sect. 3 presents a fully implicit, direct scheme for solving the equation numerically.

2 Simple formulation of transport-limited erosion

Let us start from the interpretation of Hack's empirical relation (Eq. 3) as the fingerprint of uniform erosion under spatially constant conditions. Then the the sediment flux at each point of a river (Eq. 9) is the product of the erosion rate and the catchment size,

$$Q = AE = Af(A^\theta S), \tag{10}$$

https://doi.org/10.5194/esurf-2020-39
Preprint. Discussion started: 15 June 2020


Earth Surface Dynamics Discussions
Open Access
EGU

where f is the same function used for the detachment-limited model (Eq. 4). If the stream-power approach (Eq. 6) is used, the sediment flux is

$$Q = KA^{m+1}S^n. \tag{11}$$

In contrast to the more common formalism based on the flux density q (Eq. 2), these relations use the total sediment flux Q (volume per time) passing the entire cross section of a channel segment. This total flux cannot be inserted formally into the divergence operator in Eq. (2) to form a continuous differential equation. Practically, however, this is not a problem for a discrete channel network. If any pixel of the considered topography has a unique drainage direction towards a single neighbor and sediment transport follows flow direction, the respective discrete version of the divergence operator at the node i is

$$\mathrm{div}\boldsymbol{q}_i = \frac{Q_i - \sum_j Q_j}{s_i}, \tag{12}$$

where Q_i is the flux from the node i to its flow target. The sum extends over all neighbors which deliver their sediment to the node i, called donors in the following. Finally, s_i is the area of the considered node, i.e., the pixel size for a regular mesh or the area of the respective Voronoi polygon for a triangulated irregular network (TIN). On a TIN, this formulation is practically even simpler than the version based on the flux density because the lengths of the edges of the Voronoi polygons are not needed.

The simplest form of a transport-limited fluvial erosion model then reads

$$s_i \frac{\partial H_i}{\partial t} = s_i U_i - Q_i + \sum_j Q_j, \tag{13}$$

where Q_i is defined by Eq. (10) or Eq. (11).

Equation (11) was already discussed in the literature (e.g., Whipple and Tucker, 2002) in the context of equilibrium river profiles, but apparently never used directly for defining a transport-limited erosion model. In view of Hack's findings this is, however, as straightforward as describing detachment-limited erosion by Eq. (4) or Eq. (6). Even the meaning of the erodibility K is the same in both models, so that estimates of K inferred from measurements can be used the same way in both models. The only difference is that K is a catchment-wide erodibility (obtained by averaging the erosion rates over the upstream catchment), while it is a local property in the detachment-limited model. However, it should be kept in mind that K also carries information about the entire upstream catchment in the detachment-limited model if precipitation varies within the catchment. From a process-oriented point of view, K would rather be considered a transport coefficient than an erodibility. However, this is just a matter of terminology where the term erodibility has already been used.

3 A fully implicit numerical algorithm for transport-limited erosion

The model proposed in the previous section can be treated with an efficient, fully implicit numerical scheme in the linear case ($n = 1$). The reason why this is possible in contrast to the 2-D diffusion equation lies in the tree structure of the flow and sediment transport pattern.

https://doi.org/10.5194/esurf-2020-39
Preprint. Discussion started: 15 June 2020


Earth Surface Dynamics Discussions
Open Access
EGU

The fully implicit discretization of Eq. (13) reads

$$s_i \frac{H_i(t) - H_i(t_0)}{\delta t} = s_i U_i - Q_i(t) + \sum_j Q_j(t), \tag{14}$$

where the time step extends from t_0 to t and $\delta t = t - t_0$. The solution at t_0 is known, and the solution at t is computed. Let the node b be the flow target of the node i, so H_b serves as a base level for the node i. As the entire problem is linear, the sediment flux Q_i to the node b responds linearly to base level changes and can therefore be written in the form

$$Q_i(t) = Q_i^0 + Q_i' \left(H_b(t) - H_b(t_0)\right). \tag{15}$$

Here, Q_i^0 is the flux that occurs if the base level H_b remains constant ($H_b(t) = H_b(t_0)$), and Q_i' is the derivative of $Q_i(t)$ with regard to base level changes. Inserting Eq. (15) for the donors into Eq. (14) yields

$$s_i \frac{H_i(t) - H_i(t_0)}{\delta t} = s_i U_i - Q_i(t) + \sum_j Q_j^0 + \sum_j Q_j' \left(H_i(t) - H_i(t_0)\right) \tag{16}$$

and thus

$$Q_i(t) + \frac{\alpha_i}{\delta t} \left(H_i(t) - H_i(t_0)\right) = \beta_i \tag{17}$$

with the terms

$$\alpha_i = s_i - \delta t \sum_j Q_j' \quad \text{and} \quad \beta_i = s_i U_i + \sum_j Q_j^0 \tag{18}$$

introduced in order to keep the equations short. The channel slope at the node i is

$$S_i(t) \; = \; \frac{H_i(t) - H_b(t)}{d_i}, \tag{19}$$

where d_i is the distance between the nodes i and b. So the sediment flux is

$$Q_i(t) \; = \; K A_i^{m+1} \frac{H_i(t) - H_b(t)}{d_i} \tag{20}$$

according to Eq. (11) for $n = 1$. This leads to

$$H_i(t) = H_b(t) + \frac{d_i}{K A_i^{m+1}} Q_i(t). \tag{21}$$

Inserting this relation into Eq. (17) yields

$$Q_i(t) + \frac{\alpha_i}{\delta t} \left(\frac{d_i}{K A_i^{m+1}} Q_i(t) + H_b(t) - H_i(t_0) \right) = \beta_i, \tag{22}$$

which can be rearranged in the form

$$Q_i(t) = \frac{\alpha_i \left(H_i(t_0) - H_b(t)\right) + \beta_i \delta t}{\alpha_i \frac{d_i}{K A_i^{m+1}} + \delta t}. \tag{23}$$

https://doi.org/10.5194/esurf-2020-39
Preprint. Discussion started: 15 June 2020


Earth Surface Dynamics Discussions
Open Access
EGU

Comparing this expression with Eq. (15) yields

$$Q_i^0 = \frac{\alpha_i \left(H_i(t_0) - H_b(t_0)\right) + \beta_i \delta t}{\alpha_i \frac{d_i}{K A_i^{m+1}} + \delta t} \tag{24}$$

and

$$Q_i' = -\frac{\alpha_i}{\alpha_i \frac{d_i}{K A_i^{m+1}} + \delta t}. \tag{25}$$

Equations (24) and (25) allow for the computation of Q_i^0 and Q_i' from the respective values of the donors and from known elevation values at time t_0. All values Q_i^0 and Q_i' can thus be computed successively in downstream direction. As the required order of the nodes is the same as for computing the catchment sizes A_i, it is most efficient to calculate Q_i^0 and Q_i' in the same sweep over the nodes where the catchment sizes are computed.

Once the values Q_i^0 and Q_i' have been computed for all nodes, the sediment flux $Q_i(t)$ can be computed using Eq. (15). This sediment flux is then used for computing the elevation $H_i(t)$ from Eq. (21). As these steps require the elevation of the flow target $H_b(t)$, they have to be performed successively in upstream order. This order is the same as used in the implicit scheme for detachment-limited erosion.

So the numerical scheme consists of three sweeps over the grid:

Sweep 1: Compute the flow directions b of all nodes. The nodes can be processed in any order.

Sweep 2: Compute the catchment size A and the properties Q^0 (Eq. 24) and Q' (Eq. 25) of all nodes. The nodes have to be processed in downstream order, e.g., by a recursive implementation.

Sweep 3: Compute $Q(t)$ according to Eq. (15) and $H(t)$ from Eq. (21) for all nodes. The nodes must be processed in upstream order, e.g., by a recursive implementation.

The scheme is a direct scheme without any iterative component. The derivatives Q' are always negative (lower base level leads to a higher sediment flux), so that the properties α and thus the denominator in Eqs. (24) and (25) are always positive. So the scheme is unconditionally stable, and its time complexity is linear ($O(n)$) under all conditions.

The workflow with the three sweeps is basically the same as in the implicit scheme for detachment-limited erosion. The structure is the same without any extra loops, conditions or functions to be invoked. Additional effort only arises from floating-point operations. Table 1 provides an estimate of the time complexity compared to detachment-limited erosion. All results were obtained using the landform evolution model OpenLEM that was used in some previous studies (e.g., Robl et al., 2017; Wulf et al., 2019; Hergarten, 2020), but has not been published explicitly. A regular 5000×5000 grid was used, and CPU time was normalized to the total effort of one time step for detachment-limited erosion. The difference in time complexity between both models is marginal.

With regard to memory complexity, the scheme presented here requires two additional variables per node, Q^0 and Q'. When performing the third sweep, one of them can be recycled for storing the original surface height $H(t_0)$ that is needed later when Eq. (15) is applied to the donors. The remaining variable can be used for storing the actual sediment flux $Q(t)$ in case it is needed later.

https://doi.org/10.5194/esurf-2020-39
Preprint. Discussion started: 15 June 2020

Earth Surface Dynamics Discussions
Open Access
EGU

Table 1. Time complexity of the scheme for transport-limited erosion compared to the implicit scheme for detachment-limited erosion. CPU time was normalized to the total effort of one time step for detachment-limited erosion.

	Detachment limited		Transport limited	
	properties	CPU time (%)	properties	CPU time (%)
sweep 1	b	38	b	38
sweep 2	A	49	A, Q^0, Q'	54
sweep 3	H	13	Q, H	20
total		100		112

4 A numerical example

As comparing detachment-limited and transport-limited erosion in detail would go beyond the scope of this study, only a simple example of steady-state topographies is given here. Investigating the temporal behavior turned out to be quite complex in preliminary experiments and will be subject of further studies.

The example presented here uses a square domain of 5000×5000 nodes. The northern and southern boundaries are kept at $H = 0$, while the two other boundaries are periodic. All horizontal lengths and areas are measured in terms of pixels. An exponent $m = 0.5$ was assumed, so that equilibrium rivers have a concavity index of $\theta = 0.5$ for the linear model ($n = 1$). The erodibility was set to $K = 1$.

Equilibrium topographies were computed by starting with small increments δt that are increased through time. At large δt, smaller random values of δt are used in each second step in order to avoid periodic oscillations between topographies with different flow patterns that prevent the topography from reaching a steady state.

An equilibrium topography obtained for uniform uplift $U = 1$ was used as a reference. This topography (Fig. 1, left) was generated by starting from a flat initial topography with a small random disturbance. As the transport-limited and the detachment-limited models are equivalent for uniform erosion, this topography is an equilibrium topography for both models.

As a simple non-uniform uplift pattern, tent-shaped uplift is considered. The maximum uplift rate $U = 1$ is achieved here in the middle between the northern and southern boundary ($x_2 = 2500$) and decreases linearly to zero towards the boundaries. In order to get similar flow patterns (Fig. 1), the equilibrium topography corresponding to constant uplift was used as an initial condition.

Figure 2 shows swath profiles through the three topographies. The maximum surface height (uppermost curve of the respective color) is dominated by the steep slopes at small catchment sizes. Since these depend on the local uplift rate in equilibrium, the maximum elevation roughly follows the tent-shaped uplift pattern with minor differences between transport-limited and detachment-limited erosion. The absolute difference between the two models is similar for maximum, mean, and minimum elevation, so it can be attributed to the different heights of large valleys, while local relief is similar.

The profiles of the large rivers marked in Fig. 1 are shown in Fig. 3. For a clearer representation, the longitudinal coordinate was χ transformed according to Eq. (7) with $A_0 = 1$. With the value $K = 1$ used here, equilibrium profiles follow a straight

https://doi.org/10.5194/esurf-2020-39
Preprint. Discussion started: 15 June 2020

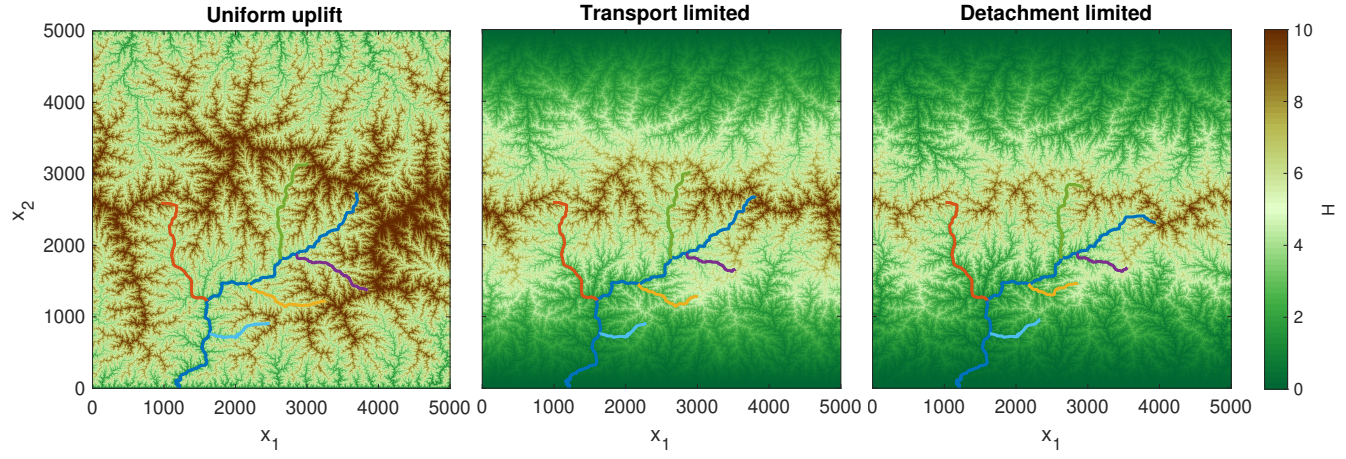

Figure 1. Equilibrium topographies for uniform uplift (left) and for a tent-shaped uplift pattern (middle and right). The color-coded rivers are the largest stream and its 5 largest tributaries in the topography for uniform uplift. They are referred to in Fig. 3.

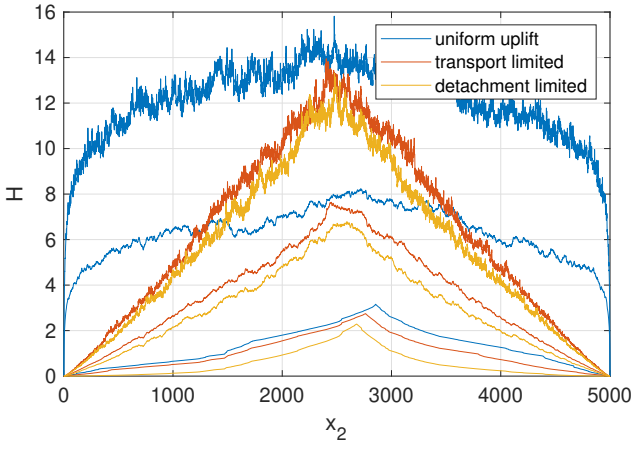

Figure 2. Swath profiles through the topographies shown in Fig. 1. The three lines of each color describe maximum, mean, and minimum elevation in east-west direction, i.e., over all values of x_1.

line $H = \chi$ at a uniform uplift rate $U = 1$. In turn, χ-transformed equilibrium profiles are concave if the uplift rate increases in upstream direction. This concavity is weaker for the transport-limited model than for the detachment-limited model as the local slope reflects the mean erosion rate of the upstream catchment, while it reflects the local erosion rate for detachment-limited erosion. In the upper part of the catchment, however, both turn into parallel straight lines. In the lower part of the catchment, the river profiles of the transport-limited model are steeper than those of the detachment-limited model because the river also has to carry away the material from the upper part with high erosion rates.

While the χ-transformed river profiles of the transport-limited model are more straight than for detachment-limited erosion, local collinearity of tributaries is lost. For detachment-limited erosion, profiles of tributaries start with the same slope as the

https://doi.org/10.5194/esurf-2020-39
Preprint. Discussion started: 15 June 2020

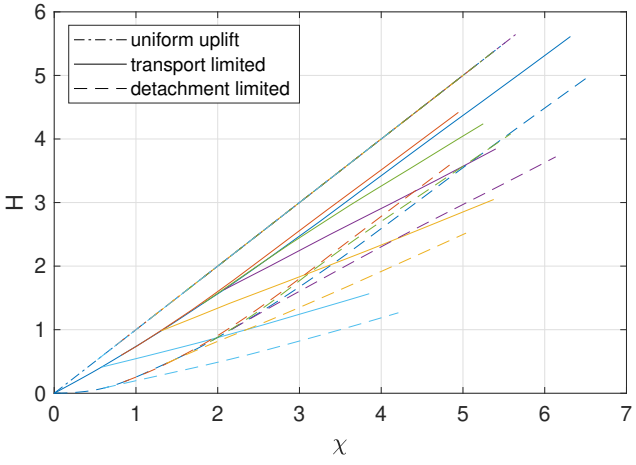

Figure 3. Longitudinal profiles of the rivers marked in Fig. 1 plotted in χ representation.

trunk stream and deviate more and more with increasing distance. In contrast, tributaries and the trunk stream may contribute different amounts of sediment per catchment size due to different mean erosion rates in their upstream catchments, which leads to different slopes immediately above the point of confluence in the transport-limited model. As a consequence, the capture of tributaries leads to stable knickpoints in the trunk stream for transport-limited erosion.

5 Combination with detachment-limited erosion

The numerical scheme described in Sect. 3 can be extended towards detachment-limited erosion at least in two ways. First, it can be transferred to linear decline models. Second, the sum of two erosion processes can be considered where a sediment balance is taken into account only for a part of the eroded material, while the rest is immediately excavated. In both cases, however, only the linear version with regard to H ($n = 1$) can be implemented as a direct solver, while nonlinearity requires either a mixed scheme (some dependencies considered at t_0 instead of t) or an iterative treatment.

5.1 Application to linear decline models

The general form of a linear decline model where the fluvial incision term is also linear reads

$$E = \phi S - \psi Q, \tag{26}$$

where S is channel slope and Q is sediment flux. The functions ϕ and ψ may depend on all properties except for surface heights (and consequently also channel slopes) in order to maintain the linearity. The first term is either related to the equilibrium sediment flux (transport capacity) in the formulation of Kooi and Beaumont (1994) or to the incision term in the concept proposed by Davy and Lague (2009). Accordingly, the second term is interpreted as deposition of particles by Davy and Lague (2009).

https://doi.org/10.5194/esurf-2020-39
Preprint. Discussion started: 15 June 2020


Earth Surface Dynamics Discussions
Open Access
EGU

Inserting Eq. (26) into the general landform evolution model (Eq. 1) yields

$$\frac{\partial H_i}{\partial t} + \phi_i S_i - \psi_i Q_i - U_i = 0, \tag{27}$$

and after inserting difference quotients for time derivative and channel slope

$$\frac{H_i(t) - H_i(t_0)}{\delta t} + \phi_i \frac{H_i(t) - H_b(t)}{d_i} - \psi_i Q_i(t) - U_i = 0. \tag{28}$$

This equation can be rearranged in the form

$$H_i(t) = \frac{H_i(t_0) + \delta t \left(\frac{\phi_i}{d_i} H_b(t) + \psi_i Q_i + U_i \right)}{1 + \frac{\delta t \phi_i}{d_i}}. \tag{29}$$

Plugging this result into Eq. (17), rearranging the resulting equation to yield $Q_i(t)$, and comparing the obtained expression to Eq. (15) finally yields

$$Q_i^0 = \frac{\alpha_i \left(\frac{\phi_i}{d_i} \left(H_i(t_0) - H_b(t_0) \right) - U_i \right) + \beta_i \left(1 + \frac{\delta t \phi_i}{d_i} \right)}{\alpha_i \psi_i + 1 + \frac{\delta t \phi_i}{d_i}} \tag{30}$$

and

$$Q_i' = -\frac{\alpha_i \frac{\phi_i}{d_i}}{\alpha_i \psi_i + 1 + \frac{\delta t \phi_i}{d_i}}. \tag{31}$$

The scheme is very similar to that presented in Sect. 3 for transport-limited erosion. Equations (30) and (31) have to be used in sweep 2. Sweep 3 is now based on Eq. (29), while Eq. (15) is still used in its original form.

For the linear version of the formulation by Davy and Lague (2009), the expressions in Eq. (26) are

$$\phi = K A^m \quad \text{and} \quad \psi = \frac{G}{A} \tag{32}$$

where G is the coefficient of deposition as used by Yuan et al. (2019) for constant precipitation, equivalent to Θ used by Davy and Lague (2009). However, it was already stated by Yuan et al. (2019) that sediment deposition makes equilibrium river profiles by a factor of $1 + G$ steeper. Assuming a uniform erosion rate and inserting $Q = EA$ into Eq. (26), it is immediately recognized that

$$(1 + G)\, E = \phi S. \tag{33}$$

So the erosion rate is indeed by a factor of $1 + G$ lower than without sediment deposition. Thus, Eq. (32) is appropriate if K is seen as a parameter of detachment-limited erosion. In turn, if K is interpreted as the fingerprint of spatially uniform erosion including sediment transport, the definition

$$\phi = (1 + G)\, K A^m \quad \text{and} \quad \psi = \frac{G}{A} \tag{34}$$

would be more useful.

https://doi.org/10.5194/esurf-2020-39
Preprint. Discussion started: 15 June 2020


Earth Surface Dynamics Discussions
Open Access
EGU

This version provides a model where the parameter G controls the transition from the detachment-limited model for $G = 0$ to the transport-limited model for $G \to \infty$ without changing the relation between K and river steepness. The numerical scheme turns into the implicit scheme for detachment-limited erosion for $G = 0$, where the flux-related variables Q^0, Q', and $Q(t)$ are computed in each time step, but are not needed for computing $H(t)$. In the opposite limit ($G \to \infty$) the scheme approaches the scheme for the transport-limited case developed in Sect. 3.

Preliminary numerical tests revealed that the time complexity of this version is very close the transport-limited case, while that of the iterative scheme proposed by Yuan et al. (2019) is close to of the detachment-limited case in each iteration step. In the first iteration, sweep 2 computes the catchment sizes here, while it integrates the upstream erosion rate to yield the sediment flux (Eq. 9) in subsequent iterations. Taking the values from Table 1, this yields 112 % vs. 162 % effort if the iterative scheme requires only two iterations (less is impossible if the flow directions change). So the direct scheme is at least 30 % faster than the iterative procedure. If the iterative scheme requires 10 iterations, the direct scheme is already 6 times faster and has the additional advantage of an exact solution without the need for checking convergence.

5.2 Adding transport-limited and detachment-limited erosion

While linear decline models can bee seen as some kind of finite transport distance for all particles, another option is to assume that a part of the eroded material is immediately excavated, while the rest is described by the transport-limited model. The linear version of this model reads

$$E = \mathrm{div}\boldsymbol{q} + \Gamma S, \tag{35}$$

or inserted into Eq. (1) and discretized in fully implicit form

$$s_i \frac{H_i(t) - H_i(t_0)}{\delta t} = s_i U_i - Q_i(t) + \sum_j Q_j(t) - s_i \Gamma_i S_i. \tag{36}$$

Here, Γ is any function that describes the excavation of material. Similarly to the functions ϕ and ψ used in the previous section, Γ may depend on all properties except for surface heights in order to maintain the linearity. It may be tempting to use $\Gamma = \tilde{K} A^m$ in analogy to the detachment-limited model, where $\tilde{K}$ has the same meaning and physical unit as K. However, Eq. (35) combines a sediment balance with immediate excavation, which causes a scaling problem if rivers are considered as linear objects (Howard, 1994; Perron et al., 2008; Pelletier, 2010; Hergarten, 2020). As a consequence, an additional rescaling factor depending on the pixel size must be introduced in the definition of Γ in order to avoid an artificial dependence of the results on the spatial resolution. Different approaches for this scaling factor are discussed in the above references.

Apart from this scaling problem, the numerical implementation is straightforward. Using Eq. (11), the last term in Eq. (36) can be expressed as

$$s_i \Gamma_i S_i = \frac{s_i \Gamma}{K A_i^{m+1}} Q_i(t). \tag{37}$$

https://doi.org/10.5194/esurf-2020-39
Preprint. Discussion started: 15 June 2020


Earth Surface Dynamics Discussions
Open Access
EGU

This results in a factor $1 + \frac{s_i \Gamma}{K A_i^{m+1}}$ in front of $Q_i(r)$ in Eq. (17). This factor propagates to the denominator of Eqs. (24) and (25), so that we finally arrive at

$$Q_i^0 = \frac{\alpha_i \left(H_i(t_0) - H_b(t_0)\right) + \beta_i \delta t}{\alpha_i \frac{d_i}{K A_i^{m+1}} + \left(1 + \frac{s_i \Gamma}{K A_i^{m+1}}\right) \delta t} \tag{38}$$

and

$$Q_i' = -\frac{\alpha_i}{\alpha_i \frac{d_i}{K A_i^{\theta+1}} + \left(1 + \frac{s_i \Gamma}{K A_i^{m+1}}\right) \delta t}. \tag{39}$$

The further steps (Eqs. 15 and 21) remain the same.

6 Further extensions and limitations

Linear diffusion (e.g., Culling, 1960) as the simplest model of hillslope erosion can be implemented more efficiently than in the detachment-limited model because the flux components in direction of the channel network can be integrated into the implicit scheme. If D is the diffusivity and l_i the length of the edge between the node i and its flow target b, the diffusive flux in this direction is

$$Q_i^{\text{diff}} = D l_i \frac{H_i - H_b}{d_i}. \tag{40}$$

Comparing this expression to Eq. (20), it is easily recognized that the term $K A_i^{\theta+1}$ just has to be replaced by $K A_i^{\theta+1} + D l_i$ throughout the calculations of Sect. 3. The other flux components still have to be handled by an explicit scheme, but as the flux component in flow direction is the largest among all, its implicit treatment improves the stability of the diffusion term and thus increases the maximum possible time increment.

However, some limitations of the approach should also be mentioned. First, any kind of sediment transport that transfers material from one site to more than one target site destroys the tree-like topology of sediment fluxes. Such processes are thus not compatible with the implicit scheme presented here. This applies, e.g., to hillslope processes as well as to fluvial processes with multiple flow directions as implemented, e.g., in the model TTLEM (Campforts et al., 2017). However, the implicit scheme for detachment-limited erosion is subject to the same limitation.

Concerning numerics, nonlinearity is the only point where the approach suggested here falls behind the implicit scheme for detachment-limited erosion. The latter can be solved directly for $n = 1$ and for $n = 2$ (Hergarten, 2002), but can be treated by finding the roots of a scalar nonlinear equation at each point for any value of n. In contrast, nonlinearity can only be included in the approach proposed here either by treating the nonlinear terms in an explicit manner or to use an iteration.

Finally, the treatment of lakes, i.e., local depressions in the topography, is a problem. In the detachment-limited model, local depressions result in negative channel slopes and thus in negative erosion rates without any specific treatment. However, these negative erosion rates can be cut off easily in the implicit scheme. In the transport-limited model, local depressions result in a sediment flux opposite to the flow direction. Erosion of dams may be too fast then, so that the lifetime of lakes may be too short. This effect cannot be fixed easily in the fully implicit scheme.

https://doi.org/10.5194/esurf-2020-39
Preprint. Discussion started: 15 June 2020

7 Conclusions

This study proposes a simple formulation of transport-limited fluvial erosion. This formulation can be immediately reconciled with the empirical results of Hack (1957) on longitudinal river profiles. The interpretation of Hack's findings as the fingerprint of spatially uniform erosion is equivalent for transport-limited erosion and for detachment-limited erosion where it has been widely used. In particular, the main properties – concavity index and erodibility – are fully equivalent in both concepts.

As a main point, a new numerical scheme for treating transport-limited erosion with a fully implicit discretization in time was presented. It is a direct solver without any iteration and is unconditionally stable for arbitrarily large time increments. It is of linear time complexity ($O(n)$) where the computing effort is marginally higher than for detachment-limited erosion. The scheme can also be applied to combined linear models of detachment-limited erosion and sediment transport such as the linear decline model. Here it also allows for approaching the transport-limited case without any loss of performance and provides a numerical efficiency that is better than the iterative scheme suggested by Yuan et al. (2019).

Code and data availability. All codes and computed data can be downloaded from http://hergarten.at/repo.zip (preliminary location during the review phase). The author is happy to assist interested readers in reproducing the results and performing subsequent research.

Author contributions. N/A

Competing interests. The author declares that there is no conflict of interest.

https://doi.org/10.5194/esurf-2020-39
Preprint. Discussion started: 15 June 2020

References

Braun, J. and Willett, S. D.: A very efficient O(n), implicit and parallel method to solve the stream power equation governing fluvial incision and landscape evolution, Geomorphology, 180–181, 170–179, https://doi.org/10.1016/j.geomorph.2012.10.008, 2013.

Campforts, B., Schwanghart, W., and Govers, G.: Accurate simulation of transient landscape evolution by eliminating numerical diffusion: the TTLEM 1.0 model, Earth Surf. Dynam., 5, 47–66, https://doi.org/10.5194/esurf-5-47-2017, 2017.

Coulthard, T. J.: Landscape evolution models: a software review, Hydrol. Process., 15, 165–173, https://doi.org/10.1002/hyp.426, 2001.

Culling, W.: Analytical theory of erosion, J. Geol., 68, 336–344, https://doi.org/10.1086/626663, 1960.

Davy, P. and Lague, D.: Fluvial erosion/transport equation of landscape evolution models revisited, J. Geophys. Res. Earth Surf., 114, F03 007, https://doi.org/10.1029/2008JF001146, 2009.

Duvall, A. R. and Tucker, G. E.: Dynamic ridges and valleys in a strike-slip environment, J. Geophys. Res. Earth Surf., 120, 2016–2026, https://doi.org/10.1002/2015JF003618, 2015.

Eizenhöfer, P. R., McQuarrie, N., Shelef, E., and Ehlers, T. A.: Landscape response to lateral advection in convergent orogens over geologic time scales, J. Geophys. Res. Earth Surf., 124, 2056–2078, https://doi.org/10.1002/2019JF005100, 2019.

Ferrier, K. L., Perron, J. T., Mukhopadhyay, S., Rosener, M., Stock, J. D., Huppert, K. L., and Slosberg, M.: Covariation of climate and long-term erosion rates across a steep rainfall gradient on the Hawaiian island of Kaua´i, GSA Bull., 125, 1146–1163, https://doi.org/10.1130/B30726.1, 2013.

Flint, J. J.: Stream gradient as a function of order, magnitude, and discharge, Water Resour. Res., 10, 969–973, https://doi.org/10.1029/WR010i005p00969, 1974.

Goren, L., Fox, M., and Willett, S. D.: Tectonics from fluvial topography using formal linear inversion: Theory and applications to the Inyo Mountains, California, J. Geophys. Res. Earth Surf., 119, 1651–1681, https://doi.org/10.1002/2014JF003079, 2014.

Hack, J. T.: Studies of longitudinal profiles in Virginia and Maryland, no. 294-B in US Geol. Survey Prof. Papers, US Government Printing Office, Washington D.C., https://doi.org/10.3133/pp294B, 1957.

Hackbusch, W.: Multi-Grid Methods and Applications, Springer, Berlin, Heidelberg, New York, https://doi.org/10.1007/978-3-662-02427-0, 1985.

Harel, M.-A., Mudd, S. M., and Attal, M.: Global analysis of the stream power law parameters based on worldwide 10Be denudation rates, Geomorphology, 268, 184–196, https://doi.org/10.1016/j.geomorph.2016.05.035, 2016.

Hergarten, S.: Self-Organized Criticality in Earth Systems, Springer, Berlin, Heidelberg, New York, https://doi.org/10.1007/978-3-662-04390-5, 2002.

Hergarten, S.: Rivers as linear elements in landform evolution models, Earth Surf. Dynam. Discuss., 2020, 1–12, https://doi.org/10.5194/esurf-2019-77, 2020.

Hergarten, S. and Neugebauer, H. J.: Self-organized critical drainage networks, Phys. Rev. Lett., 86, 2689–2692, https://doi.org/10.1103/PhysRevLett.86.2689, 2001.

Howard, A. D.: A detachment-limited model for drainage basin evolution, Water Resour. Res., 30, 2261–2285, https://doi.org/10.1029/94WR00757, 1994.

Kooi, H. and Beaumont, C.: Escarpment evolution on high-elevation rifted margins: insights derived from a surface process model that combines diffusion, advection and reaction, J. Geophys. Res., 99, 12 191–12 209, 1994.

https://doi.org/10.5194/esurf-2020-39
Preprint. Discussion started: 15 June 2020

Lague, D.: The stream power river incision model: evidence, theory and beyond, Earth Surf. Process. Landforms, 39, 38–61, https://doi.org/10.1002/esp.3462, 2014.

Pelletier, J. D.: Minimizing the grid-resolution dependence of flow-routing algorithms for geomorphic applications, Geomorphology, 122, 91–98, https://doi.org/10.1016/j.geomorph.2010.06.001, 2010.

Perron, J. T. and Royden, L.: An integral approach to bedrock river profile analysis, Earth Surf. Process. Landforms, 38, 570–576, https://doi.org/10.1002/esp.3302, 2013.

Perron, J. T., Dietrich, W. E., and Kirchner, J. W.: Controls on the spacing of first-order valleys, J. Geophys. Res. Earth Surf., 113, F04 016, https://doi.org/10.1029/2007JF000977, 2008.

Robl, J., Hergarten, S., and Prasicek, G.: The topographic state of fluvially conditioned mountain ranges, Earth Sci. Rev., 168, 290–317, https://doi.org/10.1016/j.earscirev.2017.03.007, 2017.

Royden, L. and Perron, J. T.: Solutions of the stream power equation and application to the evolution of river longitudinal profiles, J. Geophys. Res. Earth Surf., 118, 497–518, https://doi.org/10.1002/jgrf.20031, 2013.

Theodoratos, N., Seybold, H., and Kirchner, J. W.: Scaling and similarity of a stream-power incision and linear diffusion landscape evolution model, Earth Surf. Dynam., 6, 779–808, https://doi.org/10.5194/esurf-6-779-2018, 2018.

Turowski, J. M.: Semi-alluvial channels and sediment-flux-driven bedrock erosion, in: Gravel-Bed Rivers, edited by Church, M., Biron, P., and Roy, A., chap. 29, pp. 399–418, John Wiley & Sons, Ltd, https://doi.org/10.1002/9781119952497.ch29, 2012.

van der Beek, P.: Modelling landscape evolution, in: Environmental Modelling: Finding Simplicity in Complexity, edited by Wainwright, J. and Mulligan, M., pp. 309–331, Wiley-Blackwell, Chichester, 2 edn., 2013.

Whipple, K. X. and Tucker, G. E.: Dynamics of the stream power river incision model: Implications for height limits of mountain ranges, landscape response time scales and research needs, J. Geophys. Res., 104, 17 661–17 674, https://doi.org/10.1029/1999JB900120, 1999.

Whipple, K. X. and Tucker, G. E.: Implications of sediment-flux-dependent river incision models for landscape evolution, J. Geophys. Res., 107, 2039, https://doi.org/10.1029/2000JB000044, 2002.

Whipple, K. X., DiBiase, R. A., and Crosby, B. T.: Bedrock rivers, in: Fluvial Geomorphology, edited by Shroder, J. and Wohl, E., vol. 9 of *Treatise on Geomorphology*, pp. 550–573, Academic Press, San Diego, CA, https://doi.org/10.1016/B978-0-12-374739-6.00226-8, 2013.

Willgoose, G.: Mathematical modeling of whole landscape evolution, Annu. Rev. Earth Planet. Sci., 33, 443–459, https://doi.org/10.1146/annurev.ea.33.092203.122610, 2005.

Wulf, G., Hergarten, S., and Kenkmann, T.: Combined remote sensing analyses and landform evolution modeling reveal the terrestrial Bosumtwi impact structure as a Mars-like rampart crater, Earth Planet. Sci. Lett., 506, 209–220, https://doi.org/10.1016/j.epsl.2018.11.009, 2019.

Yuan, X. P., Braun, J., Guerit, L., Rouby, D., and Cordonnier, G.: A new efficient method to solve the stream power law model taking into account sediment deposition, J. Geophys. Res. Earth Surf., 124, https://doi.org/10.1029/2018JF004867, 2019.